Journal of Sciences, Islamic Republic of Iran 26(2): 153 - 161 (2015) http://jsciences.ut.ac.ir
University of Tehran, ISSN 1016-1104

Constraining the Water Activity during Peak Metamorphism in a Thermal Aureole; a Mineral Equilibria Approach

M. Moazzen*

Department of Earth Sciences, Faculty of Natural Sciences, University of Tabriz, 51664, Tabriz, Islamic Republic of Iran

Received: 1 March 2015 / Revised: 17 May 2015 / Accepted: 10 June 2015

Abstract

In order to assess the presence or absence of fluids under peak metamorphic conditions within the inner aureole of the Etive igneous complex in west Scotland, eight suitable metabasic hornfels samples and one suitable pelitic hornfels were used to calculate water activities using a mineral equilibria. Calculated activities for water are lower than unity in the pelitic sample and extremely low in the metabasic rocks. These low H_2O activities due to dilution of water by other fluid species are unlikely, since no mineralogical evidence for the presence of other fluids were found in the studied rocks. As a consequence, the low H_2O activities support fluid-absent conditions during the peak metamorphism of the inner aureole rocks. The findings from this study are in good agreement with calculated water activities using water contents of cordierite in the pelitic rocks for the same part of the aureole, suggesting that cordierite in metapelites retained its syn-metamorphic volatiles.

Keywords: Contact metamorphism; Water activity; Fluid-absent condition; Mineral equilibria.

Introduction

The presence or absence of fluids, especially water during peak metamorphic conditions is one of the most debated questions in metamorphic petrology. Assessing the role of water is very important for explaining some aspects of contact metamorphism and partial melting in thermal aureoles. There are different methods for determination of the presence or absence of water during contact metamorphic reactions. These are fluid inclusion studies, water contents of hydrous minerals and dehydration equilibria. Conventional fluid inclusion studies cannot usually be applied successfully to high-grade metamorphic rocks because most fluid inclusions in metamorphic rocks were trapped late in the rocks' histories (e. g. [26]). However some studies (e.g. [6]) show possibility of detailed analysis of fluid inclusions in metamorphic rocks. Contact aureoles may be one of the ideal environments in which to look at fluid inclusions in the metamorphic minerals. Other methods to constrain the water activity during peak metamorphic conditions are the application of water contents of water-bearing minerals, which have a water content sensitive to temperature and pressure, such as cordierite (e.g. [5, 13, 23, 28]), and calculation of the water

* Corresponding author: Tel: +984133393922; Fax: +984133250399; Email: moazzen@tabrizu.ac.ir

activity using dehydration equilibria (e.g. [10, 15, 19]). A peak metamorphic water activity close to unity is good evidence for equilibrium of minerals in the rock in the presence of aqueous fluid [15] and if the other fluid species are absent, then low values for water activity imply fluid-absent conditions (e.g. [19]). The latter method is applied to one suitable sample from the pelitic rocks and eight samples from the metabasic rocks of the Etive aureole, SW Scotland. All samples are from the high-grade inner aureole (sillimanite zone of pelitic rocks and orthopyroxene zone of metabasic rocks, [23, 24]). Breakdown of tremolite in metabasic rocks is used as mineral equilibria for water activity calculations in the metabasites as previously performed by other researchers [14]. Reaction of biotite and quartz to form garnet, K-feldspar and water in the pelitic samples is used to estimate the water activity during peak metamorphism.

Materials and Methods

The Etive igneous complex and its surrounding metasedimentary and metabasic rocks are located in the south west of Scotland in the Scottish Highlands (Fig. 1). The igneous complex is composed of a variety of igneous rocks including diorite, monzodiorite, granodiorite, granite and adamellite [1, 12, 22, 23, 24]. The complex was intruded into regionally metamorphosed metasedimentary and metavolcanic rocks of the Moine and Dalradian Supergroups during the Devonian [3]. Heat from the complex has produced a thermal aureole up to 1.5km wide [22]. Pelitic, semi-pelitic, psammitic, metabasic and calc-silicate hornfelses are the results of thermal metamorphism. Four successive mineralogical zones can be distinguished in metabasic rocks in the southern part of the Etive aureole. These are I-regional metamorphic metabasites (chlorite-actinolite zone; not present in the north Loch Awe area in Fig. 1), II-hornblende zone, III-clinopyroxene zone and IV- orthopyroxene zone. The clinopyroxene zone (zone III) can be divided into two sub-zones namely epidote-bearing and epidote-free sub-zones. The distribution of zones and isograds in the metabasic rocks is illustrated in Fig. 1. The main mineral assemblages in each zone are as follows (abbreviations from [18]).

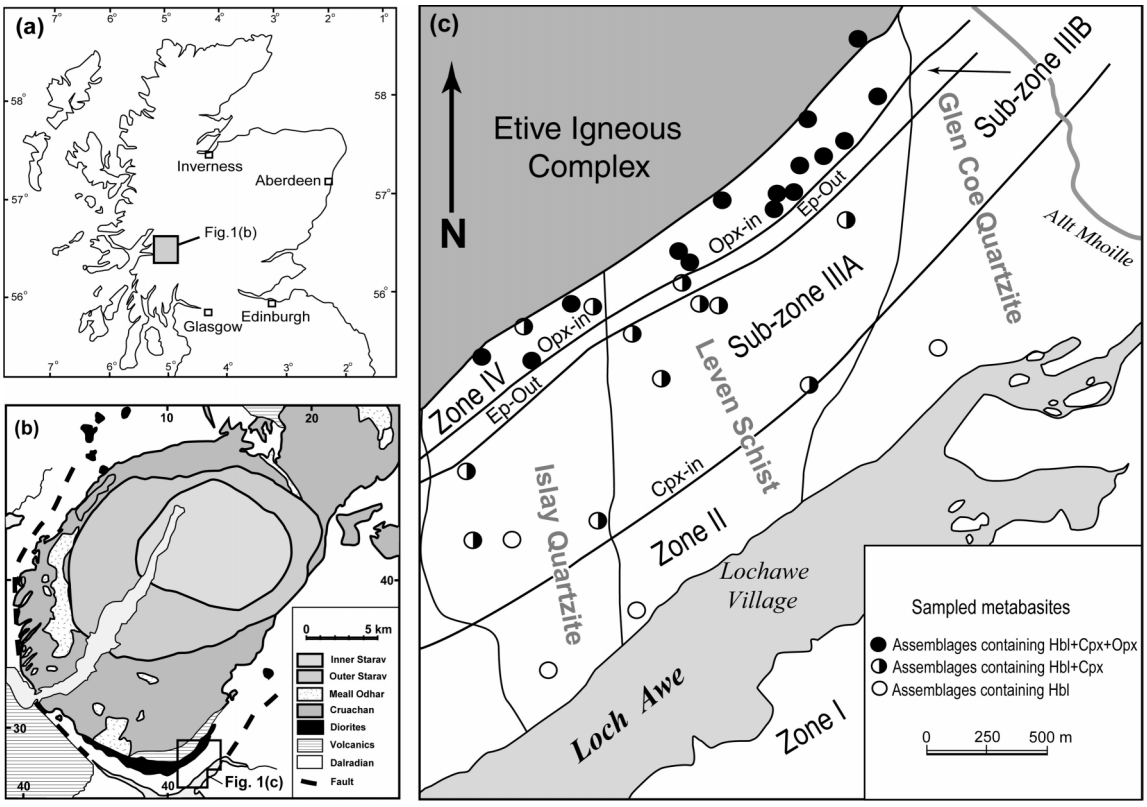

Figure 1. Distribution of sample localities, metamorphic zones and isograds in metabasites in the North Loch Awe area, SW Scotland (modified from [23 to 10]).

Zone I
Chl+Act+Pl+Ep+Qtz+Cal±Bt
Zone II
Hbl+Pl+Bt±Chl+Qtz
Zone III
Hbl+Bt+Cpx+Ep+Pl±Qtz±Czo
Hbl+Bt+Cpx+Pl+Qtz
Zone IV
Hbl+Cpx+Opx+Pl±Qtz
Hbl+Cpx+Opx+Bt+Pl±Qtz

Seven mineralogical zones are developed in thermally metamorphosed pelitic rocks [9]. Chemically suitable pelitic rocks are partially melted. Geothermobarometry of the aureole rocks using different methods [8, 9, 23, 24] and fluid conservative reactions [23] indicate a pressure of ca. 2.2kbar and a temperature of about 800°C for the orthopyroxene zone in the metabasic rocks.

Petrography

Forty five representative thin sections from the metabasic rocks were studied. Eight high-grade rocks from the orthopyroxene zone (at the vicinity of the igneous contact) contain the mineral assemblage:

Amph+Cpx+Opx+Pl+Qtz±Bt

which is potentially useful for estimation of water activity using the tremolite breakdown reaction [17]. Clinopyroxene appears as large crystals up to 1mm long with a granoblastic polygonal texture. Orthopyroxene appears as medium to coarse (up to 3mm long) elongated and occasionally skeletal crystal. Strongly pleochroic amphiboles have greenish-brown to brown colour. Idioblastic to sub-idioblastic crystals of plagioclase show polysynthetic twining and some have optical zoning. Quartz is present in the samples. Biotite can be found in some samples and shows strong pleochroism with a dark brown colour. Titanite, ilmenite, apatite and zircon are minor phases. The overall texture of the rocks is granoblastic polygonal with well-crystallized grains of hornblende, plagioclase and pyroxene.

The pelitic sample containing the necessary mineral phases for water activity calculations (sample MM166A) is a fine- to medium-grained migmatitic hornfels. The mineral assemblage is:

Grt+Crd+Bt+Kfs+Pl+Qtz

Secondary muscovite, apatite, ilmenite and zircon are minor phases. Small amounts of green spinel can be seen as inclusions in cordierite. Indistinct leucosome, rich in Kfs+Qtz (average size ca. 0.5 mm) alternate on a 2-3 mm scale with a finer-grained Crd-rich mesosome, forming stripes that follow the former S2 crenulation cleavage (deformation was during regional metamorphism, prior to contact metamorphism). Veinlets of quartz and K-feldspar with euhedral to subhedral crystals of K-feldspar and interstitial-xenomorphic crystals of quartz, which are interpreted as leucosomes crystallized from an anatectic melt, are present in this sample [22. 23]. Garnet forms relatively inclusion-free euhedral to subhedral crystals up to 2 mm across, and mainly lies within mesosome. Cordierite is abundant and occurs both as euhedral to subhedral twinned crystals, especially in leucosomes, and as elongated granoblastic polycrystalline patches aligned parallel to leucosomes. The cordierite patches commonly contain ilmenite and biotite inclusions, and locally have clusters of tiny green spinel granules. Biotite forms randomly oriented flakes up to 0.5 mm long. K-feldspar occurs as granoblastic polygonal to blocky subhedral crystals of microcline and microperthite, mostly within the leucosomes. Quartz is mostly granoblastic, but locally forms cuspate grains interstitial to blocky K-feldspar in leucosomes.

Mineral chemistry

In order to identify the chemical composition of high-grade metabasites, calculation of activity of end-members and eventually calculation of water activity during peak metamorphic conditions, minerals in eight thin sections of metabasites were analysed for major elements using electron microprobe. A modified Cambridge Instrument® Geoscan microprobe at the department of Earth Sciences in the Manchester University was used for analysis. The machine is interfaced to an Oxford Instrument®/Link Analytical QX-2000 energy dispersive X-ray spectrometer (EDS). The Link System ZAF4/FLS software was used to convert X-ray spectra obtained from the specimen into chemical analyses. A 15kv electron beam acceleration voltage and a 40 second acquisition time per analyse was applied. Under these circumstances, the detection limit is approximately 0.2 wt%. More than ten spots for each mineral were analysed in a thin section. Since the mineral chemistry of amphibole and pyroxene in metabasites are sufficient for calculation of water activity, therefore we will not consider the chemistry of other minerals in the studied samples. Quartz is considered to be pure SiO_2 in all samples.

Table 1 includes representative microprobe analyses of amphibole, clinopyroxene and orthopyroxene in metabasic rocks of the Etive thermal aureole. Amphiboles appear to be homogeneous in all analysed samples. Formula is calculated to 23 oxygen atoms and Fe^{3+} contents estimated on charge balance criteria [7]. The amphibole analyses have oxide totals of between

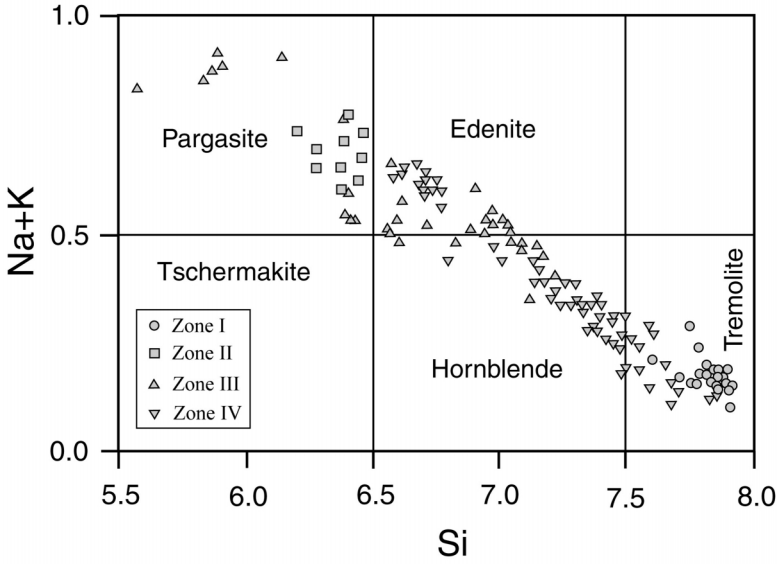

Figure 2. Classification of amphiboles in metabasites using Leake [20] diagram. All amphiboles from zone IV (orthopyroxene-clinopyroxene zone) plot in the hornblende and edenite fields.

96.13% and 98.52%. Cation totals lie between 15.12 and 15.64. Fig. 2 shows the classification of amphiboles using the diagram of [20]. No F and Cl were detected in the analysed amphiboles. Amphiboles in high-grade rocks of Zone IV plot mainly in hornblende field of the diagram.

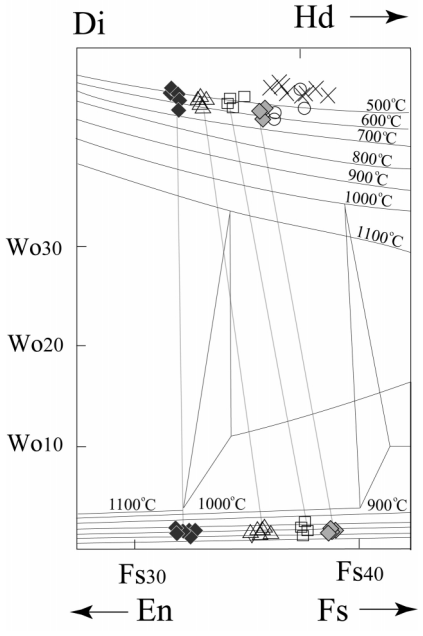

Figure 3. Wo-En-Fs diagram showing the end-member molecular proportion in orthopyroxenes and clinopyroxenes from metabasic rocks. Tie lines connect the average composition of orthopyroxene and clinopyroxene in individual samples. Isotherms showing the temperature are from [21].

Clinopyroxene formulae were calculated to 6 oxygen atoms and cation totals assumed to be exactly 4.00 [7] (Table 1). All clinopyroxenes appear to be compositionally homogeneous (i.e. without zoning). Manganese and chromium are absent in clinopyroxene or occur in very low concentrations. Calcium varies from 0.84 to 0.95 atoms per formula unit (apfu). Octahedral aluminium accounts for zero to 0.02 apfu on the M_1-site. Fe^{3+} concentration, which is estimated using charge-balance criteria [7], is between 0.01 and 0.07 and Ti varies from zero to 0.01 apfu. Fig. 3 illustrates the composition of clinopyroxene (and co-existing orthopyroxene) from metabasic rocks (from zone III and IV) on the wollastonite-enstatite-ferrosillite diagram (Wo-En-Fs). The amount of Wo is between 43% and 46%, the amount of En is between 37% and 45% and the amount of Fs is between 14% and 25%.

All analysed orthopyroxene crystals appeared to be homogeneous. Formulae have been calculated to 6 oxygen atom and ferric iron content has been estimated on the basis of exactly 4.00 cations per formula unit. The amount of Cr, Ti, Mn and K is negligible and the amount of Na is between 0.02 and 0.05 apfu. Ca varies between 0.03 and 0.05 apfu. Ferric iron calculations yield 0.02 to 0.07 Fe^{3+} apfu. The amount of Al is between zero and 0.03 apfu. Fig.3 shows the end-

member proportions of orthopyroxene, which range from 2% to 3% Wo, 51% Ti 69% En and 28% to 47% Fs.

Table 2 includes microprobe analyses of garnet, biotite and K-feldspar in the metapelitic sample. Garnet formulae were calculated on the basis of twelve oxygen

Table 1. Representative microprobe analyses of appropriate minerals in the metabasic rocks.

Amphibole						Clinopyroxene					Orthopyroxene				
Oxides	198B	196A	166B	141B	164	198B	196A	166B	141B	164	198B	196A	166B	141B	164
SiO_2	45.36	50.83	53.80	51.47	48.27	52.27	52.66	53.18	51.93	53.22	51.88	52.69	53.62	51.96	52.31
TiO_2	2.14	1.28	0.57	0.13	1.48	0.05	0.33	0.18	0.22	0.12	0.11	0.19	0.12	0.19	0.05
Al_2O_3	8.24	4.92	2.78	3.58	6.19	0.84	0.89	0.94	0.56	0.53	0.57	0.29	0.54	0.44	0.57
Cr_2O_3	0.00	0.28	0.29	0.18	0.11	0.15	0.20	0.21	0.19	0.15	0.02	0.04	0.13	0.00	0.03
Fe_2O_3	0.00	0.00	0.00	0.00	0.00	1.40	0.99	1.53	1.17	0.80	0.95	1.09	2.37	2.63	1.77
FeO	17.35	12.45	9.41	14.38	14.12	11.30	9.64	7.53	12.59	11.09	28.30	24.75	19.95	25.38	26.25
MnO	0.00	0.01	0.03	0.25	0.00	0.00	0.10	0.07	0.32	0.08	0.14	0.03	0.00	0.42	0.20
MgO	11.35	15.35	18.30	14.41	13.78	12.41	13.94	14.97	11.89	12.60	17.25	20.04	22.97	18.26	18.20
CaO	11.18	11.11	11.36	11.21	11.06	20.96	20.90	21.12	20.83	22.06	0.99	0.83	0.84	1.18	1.14
Na_2O	1.43	1.00	0.64	0.50	1.24	0.49	0.41	0.52	0.32	0.39	0.36	0.34	0.48	0.53	0.48
K_2O	0.73	0.23	0.15	0.05	0.46	0.00	0.00	0.00	0.00	0.00	0.00	0.00	0.02	0.00	0.00
Total	97.78	97.46	97.33	99.16	96.71	99.87	100.06	100.25	100.02	101.04	100.57	100.29	101.04	100.99	100.97
	Atoms to 23 Oxygen					Atoms to 6 Oxygen					Atoms to 6 Oxygen				
Si	6.80	7.40	7.68	7.59	7.17	1.98	1.97	1.97	1.97	1.99	1.98	1.98	1.97	1.97	1.98
Ti	0.24	0.14	0.06	0.01	0.16	0.00	0.01	0.00	0.00	0.00	0.00	0.00	0.00	0.00	0.00
Al	1.46	0.84	0.47	0.62	1.08	0.04	0.04	0.04	0.02	0.02	0.03	0.01	0.02	0.02	0.02
Cr	0.00	0.03	0.03	0.02	0.01	0.00	0.00	0.00	0.01	0.00	0.00	0.00	0.00	0.00	0.00
Fe^{3+}	0.00	0.00	0.00	0.00	0.00	0.04	0.03	0.04	0.04	0.02	0.03	0.04	0.06	0.07	0.05
Fe^{2+}	2.18	1.52	1.12	1.78	1.76	0.36	0.30	0.24	0.40	0.36	0.91	0.79	0.61	0.81	0.83
Mn	0.00	0.00	0.00	0.03	0.00	0.00	0.00	0.00	0.01	0.00	0.00	0.00	0.00	0.01	0.00
Mg	2.54	3.33	3.89	3.17	3.05	0.70	0.78	0.83	0.68	0.70	0.98	1.13	1.27	1.03	1.03
Ca	1.79	1.73	1.74	1.77	1.76	0.84	0.84	0.84	0.85	0.88	0.04	0.03	0.04	0.05	0.05
Na	0.42	0.28	0.18	0.14	0.36	0.04	0.03	0.04	0.02	0.03	0.03	0.02	0.03	0.04	0.04
K	0.14	0.04	0.03	0.01	0.09	0.00	0.00	0.00	0.00	0.00	0.00	0.00	0.00	0.00	0.00
Total	15.57	15.31	15.20	15.14	15.44	4.00	4.00	4.00	4.00	4.00	4.00	4.00	4.00	4.00	4.00

atoms and Fe^{3+} contents were estimated by fixing the number of cations at 8.00. The oxide totals are between 100.09 and 101.98. The number of silicones is between 2.93 and 2.98 apfu and the number of aluminium is between 1.95 and 1.98 apfu, in both cases close to the ideal number of three and two respectively, giving good stoichiometry. Fig 4 shows the mineral composition and zoning profile across the analysed garnets in the pelitic sample.

A representative analysis of biotite is provided in Table 2. The formula has been calculated on the basis of 22 oxygen atoms considering a total of four hydroxyl,

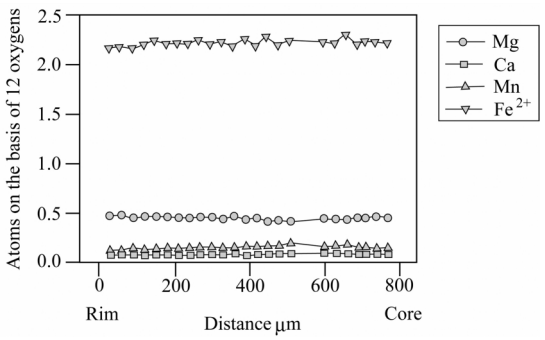

Figure 4. A zoning profile across a garnet crystal in the pelitic sample shows the homogeneity of composition.

fluorine and chlorine. The oxide totals of all biotites were between 93.36 and 96.59. The cation totals were between 14.99 and 15.01. for evaluation of F concentration in biotites, representative samples from different metamorphic zones, including sample MM166A from the sillimanite zone were analysed using the wavelength-dispersive microprobe (in the Department of Earth sciences, Manchester university). The amount of F in sample MM166A was from 0.23 to 0.47 apfu.

A representative analysis of K-feldspar is listed in Table 2. K-feldspar formulae were calculated on the basis of 8 oxygen atoms. The oxide totals were between 99.16 and 101.31. The cation totals were between 4.99 and 5.01. The proportion of orthoclase was about 80 mole percent and the anorthite content was between 0 and 1 mole percent.

Dehydration equilibria and water activity calculations

a) Dehydration equilibria in metabasic rock: Breakdown of tremolite to produce enstatite, diopside, quartz and water is used for estimation of water activity during peak metamorphism of the metabasic rocks. The reaction can be written as [17]:

$$2Tr = 3En+4Di+2Qtz+2H_2O \quad [1]$$

Thermodynamic values for end-members in reaction

Table 2. Representative analyses of minerals in the pelitic sample.

	Cordierite	Garnet	Biotite	K-feldspar
SiO_2	47.99	37.03	34.84	64.35
TiO_2	0.14	0.00	5.64	0.29
Al_2O_3	32.58	21.10	16.28	18.58
Cr_2O_3	0.03	0.09	0.16	0.05
FeO	11.77	35.67	23.29	0.04
MnO	0.17	2.06	0.00	0.13
MgO	6.57	3.83	6.92	0.00
CaO	0.05	0.87	0.04	0.00
Na_2O	0.25	0.24	0.44	1.75
K_2O	0.03	0.00	9.17	13.83
Total	99.58	100.89	96.78	99.02
Atoms	*18 (O)*	*12(O)*	*22(O)*	*8(O)*
Si	4.97	2.95	5.30	2.98
Ti	0.01	0.00	0.65	0.01
Al	3.97	1.98	2.95	1.01
Cr	0.00	0.01	0.02	0.00
Fe	1.02	2.35	3.00	0.00
Mn	0.01	0.14	0.00	0.00
Mg	1.01	0.45	1.59	0.00
Ca	0.00	0.07	0.00	0.01
Na	0.05	0.04	0.13	0.16
K	0.00	0.00	1.80	0.82
Total	11.04	7.99	15.44	4.99

[1] are provided in [17]. Data for tremolite are from experiments by Jenkins et al. [17] and the rest of the data are from Holland and Powell [16]. The equilibrium constant for reaction [1] can be written as:

$$K=(a^3_{En}.a^4_{Di}.a^2_{Qtz}.a^2_{H2O})/a^2_{Tr} \qquad [2]$$

where *a* denotes activity of a phase. The activities of enstatite in orthopyroxene and diopside in clinopyroxene were calculated using an ideal ionic model (Si-Al ordered). The activity of tremolite in amphibole was also calculated using an ideal ionic model [27]. Quartz was considered as pure phase. Calculated activities and equilibrium constant for each sample are presented in Table 3. The fugacity of water (f_{H2O}) in each sample was calculated using appropriate equation provided in [17] (See the appendix). Using the relation RTln(f_{H2O}/f^{o}_{H2O}) [29] and a polynomial expression of the PVT behaviour of H_2O following an MRK equation of state [27], the water activities in the analysed samples were calculated (R denotes the gas constant, T is temperature in Kelvin and f^o is fugacity at P and T; [4]). A pressure of 2kbar and a temperature of 800°C [23] were used in all calculations. The results are presented in Table 3.

b) Dehydration equilibria in pelitic rocks: two dehydration reactions can be considered in metapelitic sample MM166A from the lower sillimanite zone:

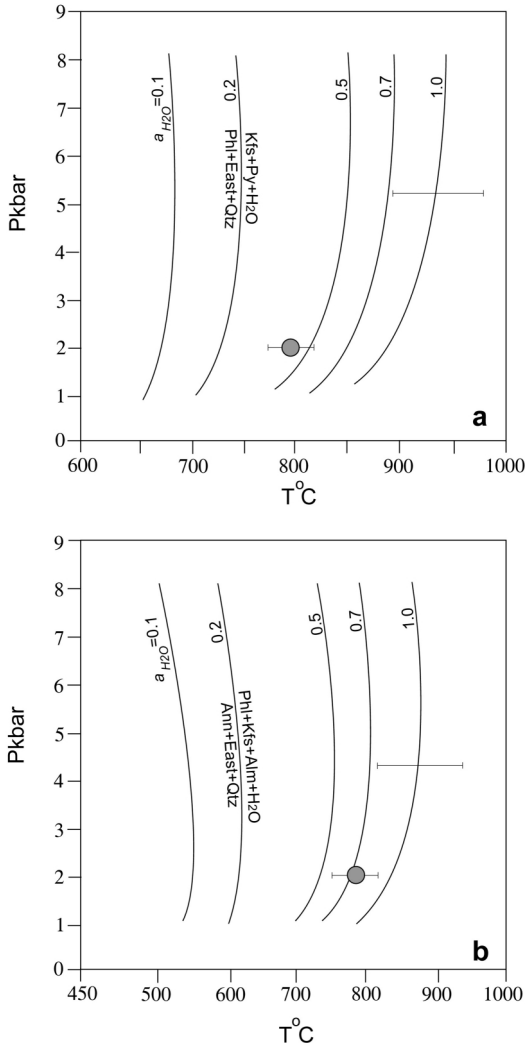

Fig. 5 Fig. 5 Estimation of water activity in the sillimanite zone garnet-bearing sample MM166A using two reactions discussed in the text. Activity of water is slightly lower than 0.5 from Fig. 5a and slightly higher than 0.7 from Fig. 5b. Both figures show water undersaturated conditions for the rocks.

$$Phl+3East+12Qtz = 4Kfs+3Py+4H_2O \qquad [3]$$
$$Ann+East+Qtz = Phl+Kfs+Alm+H_2O \qquad [4]$$

Activities of garnet end-members were calculated using the activity model of Berman [2]; whilst activities of biotite end-members were calculated using an ideal ionic model [16], and the activity of the K-feldspar end-member was calculated using the activity model of Elkins and Grove [11]. Equilibrium curves for these reactions were calculated at various water activities by the means of version 2.4 of computer software THERMOCALC [16]. The results are illustrated in Fig. 5. Considering a temperature of 800°C at 2 kbar [23],

Table 3. Activity of end-members, equilibrium constant (K), fugacities and activities of water in the studied metabasic rocks.

	198B	196A	166B	141B	164
En	0.240	0.310	0.390	0.281	0.269
Di	0.521	0.589	0.651	0.518	0.547
Tr	0.002	0.026	0.049	0.025	0.011
$K/(a^2_{H2O})$	254.64	5.304	11.491	1.1935	14.402
f_{H2O}	0.003	0.136	0.276	0.276	0.054
a_{H2O}	0.003	0.136	0.274	0.274	0.053

the rock has been equilibrated at water activities lower than 1 during peak metamorphism.

Results and Discussion

Data in Table 3 shows that water activity in metabasic rocks was low and variable (from 0.003 to 0.274). The highest water activity of 0.274 is about 1/8 total pressure (2kbar). More likely, the high variation in water activity in Table 3 is due to late retrograde hydration and if this is true, then the lowest amounts in this table are likely to be more representative for water activity at the peak of contact metamorphism in mafic rocks. It means that the water activity during high-grade contact metamorphism of mafic rocks was extremely low in the inner aureole.

The present result of the water activity study in the pelitic sample (Fig. 5) shows that this sample was also equilibrated at a water activity lower than one.

There are two possible reasons for low water activities: (i) dilution of water with other fluid species such as CO_2, NaCl, CH_4 and HF and (ii) crystallization of minerals under fluid-absent peak metamorphic conditions. Moazzen et al. [23] showed that the dilution of water by CO_2, NaCl, Hf, CH_4 and other fluids is very unlikely because there is no evidence for presence of these fluids at the peak metamorphic conditions. Therefore the low water activities reflect fluid-absent conditions.

Moazzen [22] deduced the sequence of reactions in metapelitic and metabasic rocks based on mineral parageneses and phase relations at the southern part of the Etive aureole, which involves progression from dehydration reactions in metapelites and metabasites through fluid-present partial melting to fluid-absent partial melting in pelites. Moazzen et al. [23] and Rigby et al. [28], based on water contents of cordierites, demonstrated that there was an abrupt transition in water activity in the Etive aureole to low water activities in the inner aureole, adjacent to the igneous contact. Water released from dehydration reactions in metapelites and metabasites was consumed by fluid-present melting reactions at the upper spinel zone of the pelitic assemblages. The highest grade partial melting of pelitic rocks was fluid-absent. This mechanism explains the low water activity within the inner aureole. The fluid-absent conditions for the inner aureole, which are deduced from mineral equilibria here, are in good agreement with the fluid-absent conditions concluded by Moazzen et al. [23], Rigby et al. [28] and Droop and Brodie [10].

Acknowledgements

I would like to thank Dr. G.T.R. Droop for his help and guidance and Dave Plant and Tim Hopkins from Manchester University for their assistance in microprobe analysis. Prof. Ben Harte and Prof. Simon Harley from the Edinburgh University provided valuable comments on an earlier version of the manuscript. I thank the reviewers of the journal for their perceptive reviews and Prof. Noori-Daloii for his help and encouragements. I thank Ms. Poorakbar for her enormous help during preparation of this paper.

References

1. Batchelor R. A. Geochemical and petrological characteristics of the Etive granitoid complex, Argyll. *Scot. J. Geol*., **23**:227-249 (1987).
2. Berman R.G. Mixing properties of Ca-Mg-Fe-Mn garnets. *Am. Min.,* **75**:328-344 (1990).
3. Brown P.E. Caledonian and earlier magmatism. In: *Geology of Scotland* (3rd edition). 229-295. Craig, G.Y. (ed) *Geol. Soc. London.* (1991).
4. Burnham C.W., Hollaway J.R. and Davis N.F. Thermodynamic properties of water to 1000°C and 10000 bars. *Geol. Soc. Am. Spec. Paper*, **132** (1969).
5. Carrington D. P. and Harley S.L. Cordierite as a monitor of fluid and melt H_2O content in the lower crust: An experimental calibration. *Geology*, **24**: 647-650 (1996).
6. Crawford M.L. and Hollister L.S. Metamorphic Fluids: The Evidence from Fluid Inclusions. In: *Advanc. Physic. Geochem., Fluid—Rock Interactions during Metamorphism,* Walther, J.V., Wood, B.J. (Eds.) Vol.**5** (1986).
7. Droop G.T.R. A general equation for estimating Fe^{3+} concentration in ferromagnesian silicates and oxides from microprobe analyses using stoichiometric criteria. *Min. Mag.,* **51**:431-435 (1987).
8. Droop G.T.R. and Treloar P.J. Pressure of metamorphism in the thermal aureole of the Etive Complex. *Scott. J. Geol.,* **17**:85-102 (1981).
9. Droop G.T.R. and Moazzen M. Contact metamorphism and partial melting of Dalradian pelites and semipelites in the southern sector of the Etive aureole. *Scott. J. Geol.,* **43**:

155-179 (2007).
10. Droop G.T.R. and Brodie K.H. Anatectic melt volumes in the thermal aureole of the Etive Complex, Scotland: the roles of fluid-present and fluid-absent melting. *J. Met. Geol.,* **30**:843-864 (2012).
11. Elkins L.T. and Grove T.L. Ternary feldspar experiments and thermodynamic models. *Am. Min.,* **75**:544-559 (1990).
12. Frost C.D. and O'Nions R.K. Caledonian magma genesis and crustal recycling. *J. Petrol.*, **26**:515-544 (1985).
13. Harley S.L. Cordierite as a sensor of fluid and melt distribution in crustal metamorphism. *Min. Mag.,* **58**:374-375 (1994).
14. Harlov D.E. The potential role of fluids during regional granulite-facies dehydration in the lower crust. *Geosci. Front.*, **3**:6813-827 (2012).
15. Holland T.J.B. High water activities in the generation of high pressure kyanite eclogites of the Tauern Window, Austria. *J. Geol.,* **87**:1-28 (1979).
16. Holland T.J.B. and Powell R. An enlarged and updated internally consistent thermodynamic dataset with uncertainties and correlations: the system K_2O-Na_2O-CaO-MgO-MnO-FeO-Fe_2O_3-Al_2O_3-TiO_2-SiO_2-C-H_2-O_2. *J. Met. Geol.,* **8**:89-124 (1990).
17. Jenkins D.M., Holland T.J.B. and Clare A.K. Experimental determination of the pressure-temperature stability field and thermochemical properties of synthetic tremolite. *Am. Min.,* **76**:458-469 (1991).
18. Kretz R. Symbols for rock forming minerals. *Am. Min.,* **68**:277-279 (1983).
19. Lamb W.M. and Valley J.W. Granulite facies amphibolite and biotite equilibria and calculated peak-metamorphism water activities. *Contib. Min. Pet.,* **100**:349-360 (1988).
20. Leake B.E. Nomenclature of amphiboles. *Min. Mag.,* **42**:533-563 (1978).
21. Lindsley D.H. Pyroxene thermometry. *Am. Min.,* **68**:477-493(1983).
22. Moazzen M. Contact metamorphic processes in the Etive aureole, Scotland. Unpublished Ph.D. thesis, Manchester University, 392 p (1999).
23. Moazzen M., Droop G.T.R. and Harte B. Abrupt transition in H_2O activity in the melt-present zone of a thermal aureole: Evidence from H_2O content of cordierits. *Geology*, **29(4):** 311-314 (2001).
24. Moazzen M. Tectonomagmatic characteristics of the Etive igneous complex, south west Scotland. *J. Sci. Islam. Repub. Iran,* **13(2):**141-153 (2002).
25. Moazzen M. and Droop G.T.R. Application of mineral thermometers and barometers to granitoid igneous rocks: the Etive Complex, W Scotland. *Mineral. Petrol.,* **83**:27-53 (2005).
26. Morrison J. and Valley J.W. Post-granulite facies fluid infiltration in the Adirondack Mountains. *Geology*, **16:**513-516 (1988).
27. Powell R. and Holland T.J.B. An internally consistent thermodynamic dataset with uncertainties and correlations: 1. Methods and a worked example. *J. Met. Geol.,* **3:**327-342 (1985).
28. Rigby M.J., Droop G.T.R. and Bromiley G.D. Variations in fluid activity across the Etive thermal aureole, Scotland: evidence from cordierite volatile contents. *J. Met. Geol.,* **26**:331-346 (2008).
29. Wood B.J. and Fraser D.G. Elementary thermodynamics for geologists. Oxford University Press (1977).

Appendix

Estimation of f_{H2O} in peak metamorphism of the metabasic rocks

-Reaction: Tr = 1.5En+2Di+βQtz+H_2O

-Needed variables: ΔH(J), ΔS(J/K), ΔCp (J/Kmol), ΔV(J/bar), ΔV(α)(J/K), ΔV(β)(J/K), R=8.3143 (J/Kmole)

-Equation: $\Delta G_{P,T} = \Delta H^0_{P0,T0} - T\Delta S^0_{P0,T0} + \int_{T0}^{T} \Delta C0P dT - T\int_{T0}^{T} \frac{\Delta Cp0}{T} dT + P[\Delta V^{soilds}_{P0,T0} + \Delta(\alpha V)(T - T_0) - \Delta(\beta V)P/2] + RTlnKa + RTlnf^{H2O}_{P,T}$

-Thermodynamic values for end-members (Table Appendix 1).

Activities of end-members in the mafic rocks calculated using microprobe data:

	MM198B	MM196A	MM165	MM166B	MM141B
En	0.240	0.310	0.263	0.390	0.281
Di	0.521	0.589	0.577	0.651	0.518
Tr	0.0020900	0.0262996	0.0132465	0.0494321	0.0249748

-$Ka = \frac{[En]^3[Di]^4[\beta Qtz]^2[H2O]^2}{[Tr]^2}$

-Ka :

MM198B = 233.1857385

MM196A = 5.183804045

MM166B = 11.49132472

MM141B = 2.561146356

T = 800°C = 1073°K (Opx-Cpx thermometry), P = ~2kbar [23].

$\Delta H = [1.5\ \Delta H_{En} + 2\ \Delta H_{Di} + \Delta H_{\beta Qtz} + \Delta H_{H2O}] - [\Delta H_{Tr}]$

$\Delta H_{reaction}$ = 166.49J

$\Delta V = [1.5\ \Delta V_{En} + 2\ \Delta V_{Di} + \Delta V_{\beta Qtz} + \Delta V_{H2O}] - [\Delta V_{Tr}]$

$\Delta V_{reaction}$ = -2.272 J/bar

$\Delta(\alpha V) = [1.5\ \Delta(\alpha V)_{En} + 2\ \Delta(\alpha V)_{Di} + \Delta(\alpha V)_{\beta Qtz} + \Delta(\alpha V)_{H2O}] - [\Delta(\alpha V)_{Tr}]$

$\Delta(\alpha V)_{reaction}$ = -0.000145 J/bar

$\Delta(\beta V) = [1.5\ \Delta(\beta V)_{En} + 2\ \Delta(\beta V)_{Di} + \Delta(\beta V)_{\beta Qtz} + \Delta(\beta V)_{H2O}] - [\Delta(\beta V)_{Tr}]$

$\Delta(\beta V)_{reaction}$ = -0.0155 J/bar

$Cp = a + bT + cT^{-2} + d/\sqrt{T}$

$\Delta Cp = \Delta a + \Delta bT + \Delta c/T^2 + \Delta d/\sqrt{T}$

$\Delta a = [1.5\ a_{En} + 2\ a_{Di} + a_{\beta Qtz} + a_{H2O}] - [a_{Tr}]$

$\Delta a_{reaction}$ = 86.9 J/K

$\Delta b = [1.5\ b_{En} + 2b_{Di} + b_{\beta Qtz} + b_{H2O}] - [b_{Tr}]$

$\Delta b_{reaction}$ = -0.025625 J/K

$\Delta c = [1.5\ c_{En} + 2c_{Di} + c_{\beta Qtz} + c_{H2O}] - [c_{Tr}]$

$\Delta c_{reaction}$ = 5826150 J/K

$\Delta d = [1.5\ d_{En} + 2d_{Di} + d_{\beta Qtz} + d_{H2O}] - [d_{Tr}]$

$\Delta d_{reaction}$ = -2454.85 J/K

$\Delta Cp = \Delta a + \Delta bT + \Delta c/T^2 + \Delta d/\sqrt{T}$

$\Delta Cp_{reaction}$ = -10.47722463 J/Kmol

If $A = [\Delta V^{soilds}_{P0,T0} + \Delta(\alpha V)(T - T_0) - \Delta(\beta V)P/2]$

After integration we have:

$$\Delta G_{P,T} = \Delta H^0_{P0,T0} - T\Delta S^0_{P0,T0} + [T\Delta Cp^0]^T_{T0} - T[\Delta CP^0 lnT]^T_{T0} + A + RTlnKa + RTLnf^{H2O}_{P,T}$$

A=13.112

If all phases in equilibrium, then ΔG = 0

Then: $\ln f_{H2O} = 6.561757 - \ln Ka$

Having lnKa for each ample (see above) it is possible to calculate f_{H2O} (water activity (or fugacity, water as a fluid)).

Table Appendix 1- Thermodynamic values at 298K and 1 bar. Data for tremolite are from [17] and the rest of the data are from [16].

Phase	ΔH (KJ/mol)	S (J/MolK)	V (J/bar)	Cp a	Cp b ×10^{-5}	Cp c	Cp d	αV ×10^{-5}	βV ×10^{-5}
tremolite	-12302.90	550.00	27.270	1.2144	2.6528	-12362.0	-7.3885	84.5	36.00
enstatite	-3089.38	132.50	6.262	0.3562	-0.2990	-596.9	-3.1853	18.0	4.60
diopside	-3200.15	142.70	6.619	0.3145	0.0041	-2745.9	-2.0201	22.0	5.50
β-quartz	-909.07	0.74	2.367	0.0979	-0.3350	-636.2	-0.7740	0.0	2.60
H_2O	-241.81	0.03	-	0.0401	0.8656	487.5	-0.2512	-	-